Explanation for the Absence of Secondary Peaks in Black Hole Light Curve Autocorrelations

Alejandro Cárdenas-Avendaño,[1,2,*] Charles Gammie,[3,†] and Alexandru Lupsasca[4,‡]
[1]Princeton Gravity Initiative, Princeton University, Princeton, New Jersey 08544, USA
[2]Department of Physics, Princeton University, Princeton, New Jersey 08544, USA
[3]Astronomy, Physics, NCSA, and ICASU, University of Illinois, Urbana, Illinois 61801, USA
[4]Department of Physics & Astronomy, Vanderbilt University, Nashville, Tennessee 37212, USA

(Received 13 June 2024; accepted 29 August 2024; published 27 September 2024)

The observed radiation from hot gas accreting onto a black hole depends on both the details of the flow and the spacetime geometry. The lensing behavior of a black hole produces a distinctive pattern of autocorrelations within its photon ring that encodes its mass, spin, and inclination. In particular, the time autocorrelation of the light curve is expected to display a series of peaks produced by light echoes of the source, with each peak delayed by the characteristic time lapse τ between light echoes. However, such peaks are absent from the light curves of observed black holes. Here, we develop an analytical model for such light curves that demonstrates how, even though light echoes always exist in the signal, they do not produce autocorrelation peaks if the characteristic correlation timescale λ_0 of the source is greater than τ. We validate our model against simulated light curves of a stochastic accretion model ray traced with a general-relativistic code, and then fit the model to an observed light curve for Sgr A*. We infer that $\lambda_0 > \tau$, providing an explanation for the absence of light echoes in the time autocorrelations of Sgr A* light curves. Our results highlight the importance for black hole parameter inference of spatially resolving the photon ring via future space-based interferometry.

DOI: 10.1103/PhysRevLett.133.131402

Introduction—Light emitted from hot gases accreting onto black holes has been observed for decades across the electromagnetic spectrum [1–3]. This radiation depends on both the details of the astrophysical sources and the spacetime geometry around the black holes.

More precisely, a single source around a black hole can produce multiple images arising from photons that circumnavigate the event horizon a different number of times on their way to the observer. These mirror images are lensed into a distinctive "photon ring" that represents the stamp imprinted on a black hole image by its strong gravity [4–7], and which tracks a "critical curve" [8].

Successive images appearing within the photon ring are increasingly demagnified, rotated, and time-delayed. In the simplest case of an equatorial source viewed by a distant observer on the black hole spin axis, these images accumulate near the critical curve and may be labeled by the number of polar half-orbits that the corresponding photons execute around the black hole before reaching the observer. If the nth image of a point source appears at a time t_n, at an angle φ_n around the critical curve and at a perpendicular distance d_n from it, then one can analytically prove [9] that the next image will appear at

$$t_{n+1} \approx t_n + \tau, \quad \varphi_{n+1} \approx \varphi_n + \delta, \quad d_{n+1} \approx e^{-\gamma} d_n, \quad (1)$$

where the "critical parameters" τ, δ, and γ—controlling the time delay, rotation, and demagnification of strongly lensed images, respectively—are known functions of the black hole mass and spin [9,10]. In particular, $\tau \approx 16M$ for most values of the spin, where M denotes the black hole mass and we work in geometric units with $G = c = 1$.

Because of the lensing behavior (1) of the black hole, the autocorrelation of its photon ring image intensity must display a distinctive multipeaked structure, with the heights and locations of successive peaks respectively demagnified by $e^{-\gamma}$ and shifted in the spatiotemporal correlation plane $(\Delta t, \Delta\phi)$ by (τ, δ) [11] (Fig. 1 therein).

The recent horizon-scale images taken by the Event Horizon Telescope (EHT) of the supermassive black holes M87* [12,13] and Sgr A* (the one at the center of our Galaxy) [14] are unable to resolve their photon rings. Vigorous efforts to extend the EHT array to space are now underway [15–17], and future observations using very-long-baseline interferometry to space could achieve the resolution needed to measure these rings and their predicted (ring-averaged) autocorrelations [11].

In the meantime, one can already access the black hole light curves observed over many frequencies and for many

*Contact author: cardenas-avendano@princeton.edu
†Contact author: gammie@illinois.edu
‡Contact author: alexandru.v.lupsasca@vanderbilt.edu

sources, including active galactic nuclei, x-ray binaries, and gamma-ray bursts [18–20]. Such light curves may be regarded as (single-pixel) "images" that are completely spatially averaged (over both radius and angle). Based on the preceding discussion, one would expect the temporal autocorrelation of many of these light curves to display multiple peaks, with each successive one demagnified by $e^{-\gamma}$ and delayed in time by the characteristic interval τ between light echoes [11,21–25]. However, such time autocorrelations have never been detected.

In particular, an analysis of a decade of 230 GHz light curves of Sgr A* reported a characteristic autocorrelation timescale of 8^{+3}_{-4} h at 95% confidence, present down to at least a few Schwarzschild radii [26]. Assuming a mass of $4.3 \times 10^6 M_\odot$, this value corresponds in geometric units to a timescale of $1361^{+510}_{-680} M$, which is significantly higher than the expected light echo time delay $\tau \approx 16M$. An analysis of newer data collected during the 2017 EHT observation campaign of Sgr A* reported a characteristic autocorrelation timescale of $\sim$1 h, or $\sim 170M$ [27].

Despite being significantly lower, this timescale is still much longer than the expected light echo time delay of $\tau \approx 5$ min. This raises the obvious question: where are the light echo autocorrelation peaks?

In this Letter, we revisit the theoretical expectations for the time autocorrelation of a black hole light curve and argue that the peaks caused by lensed images of the main emission are only present if the characteristic timescale λ_0 of temporal correlations in the source is much shorter than the light echo time delay τ. By contrast, if $\lambda_0 \gtrsim \tau$, then these maxima ought to be absent, even if the lensed images are present and contribute flux to the light curve.

To support this claim, we derive an analytical model for the light curve of a black hole that is surrounded by an equatorial source observed "face on" (that is, at a small inclination θ_o from the spin axis). We then argue that the model continues to hold provided the parameter $a_* \sin\theta_o$ remains small, where $a_* = J/M^2 \in [-1, 1]$ denotes the black hole spin and J its angular momentum.

We validate our model against simulated light curves of a stochastic accretion model that we ray trace using a general-relativistic code, and then we fit the model to an observed light curve for Sgr A*. We infer that $\lambda_0 > \tau$, providing an explanation for the absence of secondary peaks in the time autocorrelations of Sgr A* light curves.

Theoretical expectations—Consider a polar observer ($\theta_o = 0°$) of equatorial emission around the black hole. We decompose the full image into layers labeled by n,

$$I(t_o, \alpha, \beta) = \sum_{n=0}^{\infty} I_n(t_o, \alpha, \beta), \tag{2}$$

where the nth layer corresponds to the image of the source produced by photons that travel n half-orbits around the black hole, described in Cartesian coordinates (α, β) on the image plane at observation time t_o [8]. It is sometimes more convenient to use a polar angle φ and perpendicular distance d from the critical curve as image coordinates [9]. It follows from the lensing equations (1) that

$$I_n(t_o, \varphi, d) \approx I_{n-1}(t_o - \tau, \varphi - \delta, e^\gamma d), \tag{3}$$

up to small corrections in $1/n$ that are already negligible for $n \gtrsim 2$. Each image layer has a flux ("light curve")

$$\mathcal{L}_n(t_o) = \int I_n(t_o, \alpha, \beta) \mathrm{d}\alpha \mathrm{d}\beta. \tag{4}$$

The lensing relation (3) implies that

$$\mathcal{L}_n(t_o) \approx e^{-\gamma} \mathcal{L}_{n-1}(t_o - \tau). \tag{5}$$

Hence, the total observed light curve is approximately

$$\mathcal{L}(t_o) = \sum_{n=0}^{\infty} \mathcal{L}_n(t_o) \approx \sum_{n=0}^{\infty} e^{-n\gamma} \mathcal{L}_0(t_o - n\tau). \tag{6}$$

As expected, it consists of a superposition of multiple copies of the light curve $\mathcal{L}_0(t_o)$ of the direct emission. Each copy carries $e^{-\gamma}$ less flux and is time-delayed by τ relative to its predecessor. If the source is stationary, then the covariance $C_0(\Delta t) = \langle \mathcal{L}_0(t_o) \mathcal{L}_0(t_o + \Delta t) \rangle$ of the light curve for the direct emission is time-translation invariant, and the full light curve covariance at lag Δt [we use $\langle \mathcal{L}_i(t) \mathcal{L}_j(t + \Delta t) \rangle \approx \langle \mathcal{L}_0(t - i\tau) \mathcal{L}_0(t + \Delta t - j\tau) \rangle$ from Eq. (5), and then shift (i, j) to $(m, 2s) = (i - j, i + j - |m|)$] is

$$C(\Delta t) = \langle \mathcal{L}(t_o) \mathcal{L}(t_o + \Delta t) \rangle \tag{7}$$

$$= \sum_{i=0}^{\infty} \sum_{j=0}^{\infty} e^{-(i+j)\gamma} \langle \mathcal{L}_i(t) \mathcal{L}_j(t + \Delta t) \rangle \tag{8}$$

$$\approx \sum_{i=0}^{\infty} \sum_{j=0}^{\infty} e^{-(i+j)\gamma} C_0(\Delta t + (i - j)\tau) \tag{9}$$

$$= \frac{1}{1 - e^{-2\gamma}} \sum_{m=-\infty}^{\infty} e^{-|m|\gamma} C_0(\Delta t + m\tau), \tag{10}$$

which is also stationary. This expression agrees with the conclusions arrived at by different means in Ref. [11] and describes a train of correlation peaks separated in time by τ and exponentially decreasing in height by $e^{-\gamma}$.

As argued in Sec. 7 of Ref. [11], even though the lens equations (1) and (3) are modified for $\theta_o > 0$, the formula (10) nevertheless remains exact to leading (linear) order in $a_* \sin\theta_o$, with the first correction coming in only at subleading (quadratic) order. Thus, the only relevant time delay at small inclinations is the orbital half-period $\tau(\tilde{r}_0)$ of

the null geodesics trapped at the radius $\tilde{r}_0$ where bound photons have vanishing spin angular momentum. Likewise, the Lyapunov exponent $\gamma(\tilde{r}_0)$ governing their orbital instability fully controls the demagnification [9].

For moderate inclinations, the only meaningful change one can expect is that strongly lensed photons may skirt a range of bound orbits at different radii $\tilde{r}$ in the "photon shell" of trapped null geodesics [6]. The time delay $\tau(\tilde{r})$ and Lyapunov exponent $\gamma(\tilde{r})$ are functions of this orbital radius, so one expects a smearing of Eq. (10) over a range of $\tilde{r}$, which remains quite narrow up to $\theta_o \lesssim 45°$. At $\tilde{r}_0$, $\tau \approx 16M$ for all a_* as $e^{-\gamma}$ ranges from $e^{-\pi} \approx 4\%$ to 10%.

Therefore, we take the expression (10) (with τ and γ always evaluated near $\tilde{r}_0$) as our general analytical model for the covariance of the light curve. Since $e^{-\gamma} \lesssim 10\%$, we expand the time autocorrelation of the light curve as

$$\mathcal{C}(\Delta t) = \frac{C(\Delta t)}{C(0)} \approx \mathcal{C}_0(\Delta t)[1 - 2e^{-\gamma}\mathcal{C}_0(\tau)] + e^{-\gamma}[\mathcal{C}_0(\Delta t + \tau) + \mathcal{C}_0(\Delta t - \tau)], \quad (11)$$

where $\mathcal{C}_0(\Delta t) = C_0(\Delta t)/C_0(0)$ is the direct light curve time autocorrelation, and we have suppressed $\mathcal{O}(e^{-n\gamma})$ terms with $n \geq 2$, incurring only negligible errors $\lesssim 1\%$.

The prediction (11) is our main theoretical result. It is analytically well-motivated and we numerically validate it in the next section. Our key point is that when the direct emission has a characteristic correlation timescale $\lambda_0 \gtrsim \tau$, the expected peaks at $\Delta t \approx \tau$ in Eq. (11) vanish.

More precisely, Eq. (10) predicts correlation peaks at regular intervals $\Delta t \sim m\tau$. We now focus on the peak at $\Delta t \sim \tau$, expected to be produced by lensed images of the source whose photon half-orbit numbers differ by 1. Here, it is important to distinguish between two regimes.

The typical time autocorrelation $\mathcal{C}_0(\Delta t)$ for a source with temporal correlations on a characteristic timescale λ_0 is a monotonically decreasing function, which starts at $\mathcal{C}_0(0) = 1$ (by definition), slowly drops until $\Delta t \sim \lambda_0$, and then decays exponentially for $\Delta t \gtrsim \lambda_0$.

If $\tau \gg \lambda_0$, then $\mathcal{C}_0(\tau) \approx \mathcal{C}_0(\Delta t + \tau) \approx 0$, and thus Eq. (11) reduces to the simpler form

$$\mathcal{C}(\Delta t) \approx \mathcal{C}_0(\Delta t) + e^{-\gamma}\mathcal{C}_0(\Delta t - \tau), \quad (12)$$

describing a main peak at $\Delta t = 0$ (corresponding to the perfect autocorrelation of the signal with itself), followed by the expected secondary peak at $\Delta t = \tau$.

By contrast, if $\tau \ll \lambda_0$, then $\mathcal{C}_0(\tau) \approx 1$ and moreover, $\mathcal{C}_0(\Delta t \pm \tau) \approx \mathcal{C}_0(\Delta t)$ for lags $\tau \sim \lambda_0$, so Eq. (11) predicts

$$\mathcal{C}(\Delta t) \overset{\Delta t \sim \tau}{\approx} \mathcal{C}_0(\Delta t). \quad (13)$$

Hence, there should be no secondary peak in this regime.

As reported in the Supplemental Material (SM) [28], we observe these two behaviors in our numerical simulations. In the intermediate regime $\tau \sim \lambda_0$, we find that as τ increases, the secondary peak changes from a "bump" to an "excess" and usually disappears well before $\tau \approx \lambda_0$.

State-of-the-art simulations using general-relativistic magnetohydronamics (GRMHD) typically find accretion flows that circulate around the black hole at very slightly sub-Keplerian velocities $\Omega \approx \xi\Omega_K$, with sub-Keplerianity $\xi \lesssim 1$ [36,37]. There is also experimental evidence for such behavior from observations with GRAVITY [38].

If the characteristic timescale of correlations tracks the orbital period of the circularized flow, so that $\lambda_0 \sim 2\pi/\Omega$, then $\lambda \gg \tau$ everywhere in the gas. In light of Eq. (13), this provides an explanation for the absence of secondary peaks in observed black hole light curve autocorrelations.

Applications—We apply our model (11) for the time autocorrelation of light curves to (i) synthetic data and (ii) a light curve of Sgr A* from the 2017 EHT campaign.

For (i), we use INOISY [39] to simulate an equatorial source with stochastic fluctuations and AART [40] to ray trace its relativistic images. More exactly, we use INOISY to generate realizations of Gaussian random fields with a Matérn covariance, which serve as a proxy for a hot gas that surrounds the black hole and fluctuates with a prescribed correlation structure. We then ray trace these realizations using AART, a code that exploits the integrability of light propagation in the Kerr spacetime to efficiently produce high-resolution black hole movies.

This semianalytical approach to producing black hole movies with an analytically known covariance function is arguably the "optimal setup" for extracting echoes from light curves, since this method gives us complete control over all correlation scales and black hole parameters. See the SM for the details of the implementation [28].

We consider a Kerr black hole with spin $a_* = 94\%$ observed from an inclination $\theta_o = 20°$, and sources with different characteristic timescales λ_0. We compare their resulting autocorrelations $\mathcal{C}(\Delta t)$ to the prediction (11). The blue line in Fig. 1 (top panel) shows the light curve (6) corresponding to a Keplerian flow with $\lambda_0 = 2\pi/\Omega_K$, i.e., proportional to $r_s^{3/2}$, with r_s the equatorial radius in the source. For this position-dependent correlation time, the resulting Gaussian random field is inhomogeneous and anisotropic (see SM for an example snapshot [28]). The blue open crosses in Fig. 1 (bottom-left panel) plot the corresponding time autocorrelation, which does not present a secondary peak at $\Delta t \sim \tau$, consistent with Eq. (13) and its implications.

We stress that the absence of correlation peaks in these simulations cannot be attributed to limitations in the computation of the light curves (as we have full control of the simulation resolution and sampling rate) or in their analysis (we also applied high-pass filters and computed derivatives to search for concavity changes, to no avail).

If the source has constant correlation scales, then the light curve $\mathcal{L}_0(t_o)$ of the direct image $I_0(t_o, \alpha, \beta)$ is a

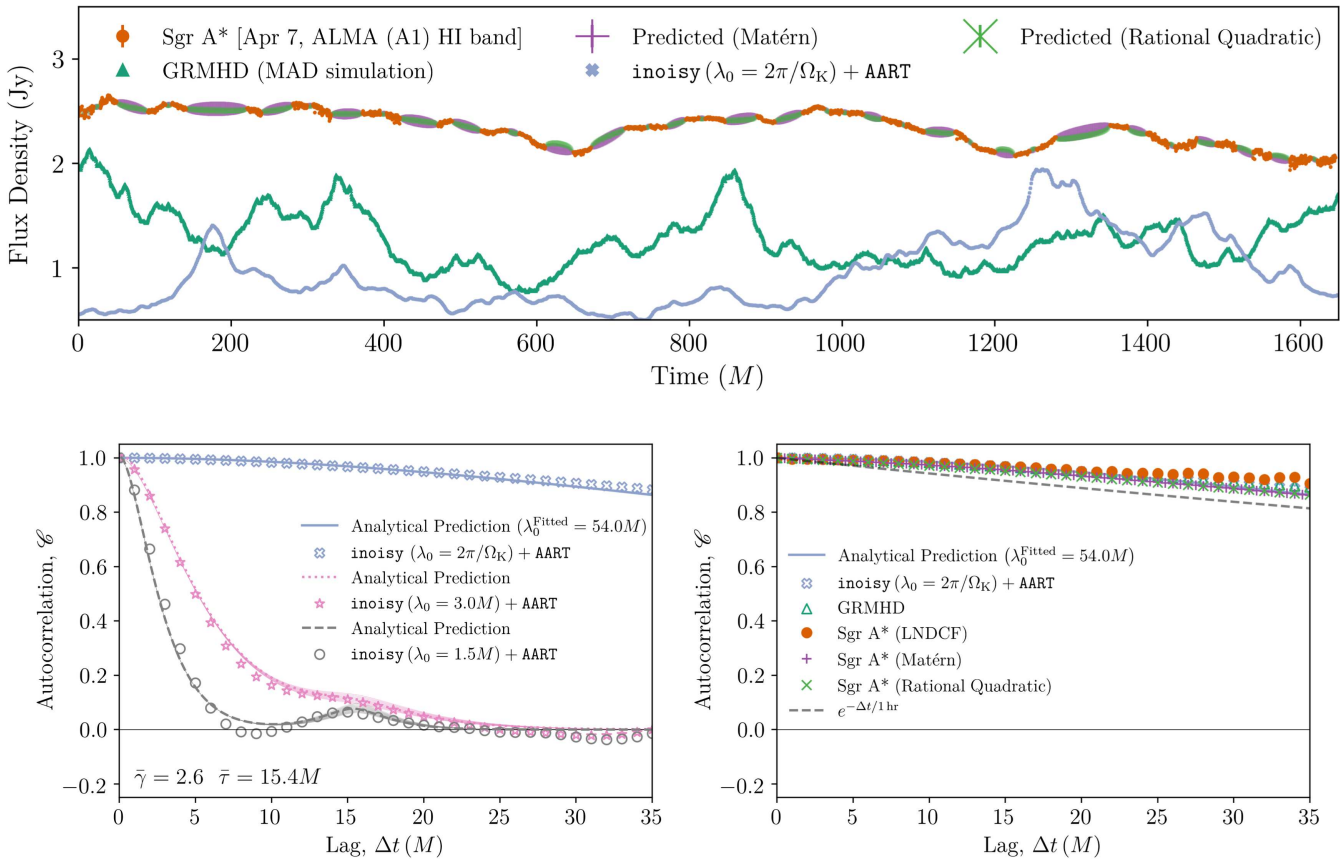

FIG. 1. Top panel: light curves from an observation of Sgr A* with ALMA [27], from a GRMHD simulation [41], and from an INOISY simulation with $\lambda_0 = 2\pi/\Omega_K$ ray traced with AART. We assumed a mass $M = 4.3 \times 10^6 M_\odot$ for Sgr A* to convert time to units of M. Bottom left: the autocorrelation of synthetic light curves produced with INOISY using different correlation times and ray traced with AART assuming a black hole with spin $a_* = 94\%$ observed from an inclination $\theta_o = 20°$. For this geometry, the Lyapunov exponent $\gamma(\tilde{r})$ ranges over [2.34, 2.79] and the time delay $\tau(\tilde{r})/M$ ranges over [15.20, 15.85], where the lower and upper bounds correspond to the innermost radius $\tilde{r}_-$ and outermost radius $\tilde{r}_+$, respectively, within the photon shell. We have used their mean values (written in the plots) for the analytical predictions presented with lines. The transparent lines represent all the possible predictions when using the whole set of values of γ and τ. The gray and pink open circles correspond to underlying correlation timescales $\lambda_0 = 1.5M$ and $\lambda_0 = 3.0M$, respectively. The blue crosses correspond to the autocorrelation of the light curve shown in the top panel computed from an INOISY and AART simulation. Bottom right: the autocorrelations of the light curves presented in the top figure. For the observed light curve of Sgr A*, we computed the autocorrelation using the LNDCF algorithm directly (orange dots), and after interpolating it with two different kernels for a Gaussian process regression (purple pluses, for Matérn, and blue crosses, for rational quadratic). The solid line corresponds to the best fit to Eq. (14) presented in the bottom-left panel. For comparison, as in Ref. [27], we include as a dashed line an exponential decay with a 1 h timescale. From these results, we infer that $\lambda_0 > \tau$, providing an explanation for the absence of light echoes in the time autocorrelation of Sgr A* light curves.

Matérn field with $d = 1$, $\nu = 3/2$ and correlation length λ_0 [28]. Its autocorrelation is

$$\mathcal{C}_0(\Delta t) = \left(1 + \frac{|\Delta t|}{\lambda_0}\right) \exp\left(-\frac{|\Delta t|}{\lambda_0}\right). \tag{14}$$

We emphasize that this is not a numerical fit to INOISY simulations, but rather the analytical formula describing the autocorrelation of the underlying stochastic model. This autocorrelation is also in agreement with our ray traced light curves, even when the observer is inclined and the black hole rotates rapidly, as shown in Fig. 1 (bottom-left panel) for two different values of λ_0. The case with $\lambda_0 = 1.5M \ll \tau$ displays a clear secondary peak (or "bump") while the case with $\lambda_0 = 3.0M < \tau$ leads only to a milder "excess" in the autocorrelation.

When the correlation timescale λ_0 varies across the source, we cannot provide an analytical expression for the resulting autocorrelation like the one in Eq. (14). We can, however, use Eq. (14) to derive an effective λ_0 by fitting it to the autocorrelation data. For the Keplerian flow with $\lambda_0 = 2\pi/\Omega_K$, we obtain a good fit with an effective $\lambda_0 = 54.0M$, as shown with the solid blue line in Fig. 1.

For (ii), we compute the autocorrelation of an observed intensity light curve for Sgr A* and call upon the intuition built from our model to interpret the results. Specifically,

we use the April 7, 2017 data from the 229.1 GHz (HI) ALMA (A1) band [27]. In Fig. 1 (top panel), we show the observed Sgr A* light curve (orange points), as well as a simulated light curve computed from an M87*-like GRMHD simulation (green triangles) of a magnetically arrested disk (MAD) with $r_{\rm high} = 40$ around a black hole with $a_* = 85\%$ and $\theta_{\rm o} = 163°$ [41]; see Refs. [41,42] for more details. To obtain an autocorrelation from the observed Sgr A* light curve, we must account for its gaps. As in Ref. [27], we compute a locally normalized discrete correlation function (LNDCF) [43,44] and use Gaussian process regression (GPR) [45] to interpolate the data. This then allows us to apply the same procedure used for the synthetic light curves. See the SM for details of these implementations [28]. The resulting autocorrelations are similar regardless of the method used to obtain them.

Although the GRMHD and INOISY + AART light curves in Fig. 1 (top panel) are produced from very different models, their time autocorrelations (bottom-right panel) are remarkably similar to each other and also to the ones computed from the observed light curve of Sgr A*.

Consistent with Ref. [27], Fig. 1 (bottom-right panel) shows no clear signs of a correlation peak at lag $\Delta t \sim \tau$ that could be interpreted as an effect of lensing by Sgr A*.

We plot the complete autocorrelation in the SM [28]. Since $\mathcal{C}(\tau) \approx 1$, the plot strongly suggests that $\lambda_0^{\rm Sgr\,A^*} > \tau$: that is, the characteristic timescale of correlations in the plasma around Sgr A* appears to exceed the time delay between light echoes. Hence, in accordance with Eq. (13), we should not expect to see secondary correlation peaks, explaining their absence from observations.

In passing, we note that the Sgr A* autocorrelation is well-approximated by the simulated autocorrelation (14) of a Keplerian flow with effective $\lambda_0 = 54.0M > \tau$ (solid blue lines in the bottom panels of Fig. 1).

Discussion—We have developed a simple analytical model for the autocorrelation of black hole light curves that offers insight into some of the challenges involved in separating the effects of the plasma from those of the spacetime geometry. When applied to an observed light curve of Sgr A*, our model suggests that the temporal correlations inherent in its surrounding plasma suppress the autocorrelation peaks expected from lensing around the black hole, explaining the absence of such signatures.

These results indicate that the inference of black hole parameters from strong lensing effects will be difficult via light curve autocorrelations alone, and likely require future space very-long-baseline interferometry observations that spatially resolve the photon ring. Planning for such observations is underway.

Acknowledgments—We thank Maciek Wielgus and George Wong for their valuable comments, and for providing the data for the Sgr A* and GRMHD light curves, respectively. We also thank Neal Dalal, Suvendu Giri, Lennox Keeble, Aviad Levis, Leo Stein, and Sam Gralla for helpful discussions. C. G. and A. L. also thank the Aspen Center for Physics, which is supported by NSF Grant PHY-2210452. A. C. A. acknowledges support from the Simons Foundation. A. L. is supported by NSF Grants AST-2307888 and PHY-2340457. C. G. was supported in part by the IBM Einstein Fellow Fund at the Institute for Advanced Study. Some of the simulations presented in this work were performed on computational resources managed and supported by Princeton Research Computing, a consortium of groups including the Princeton Institute for Computational Science and Engineering (PICSciE) and the Office of Information Technology's High Performance Computing Center and Visualization Laboratory at Princeton University.

[1] M. Schmidt, Nature (London) **197**, 1040 (1963).
[2] S. Bowyer, E. T. Byram, T. A. Chubb, and H. Friedman, Science **147**, 394 (1965).
[3] R. Narayan and E. Quataert, Nature (London) **615**, 597 (2023).
[4] J. P. Luminet, Astron. Astrophys. **75**, 228 (1979), https://articles.adsabs.harvard.edu/full/1979A%26A....75..228L.
[5] S. E. Gralla, D. E. Holz, and R. M. Wald, Phys. Rev. D **100**, 024018 (2019).
[6] M. D. Johnson, A. Lupsasca *et al.*, Sci. Adv. **6**, eaaz1310 (2020).
[7] A. Lupsasca, D. R. Mayerson, B. Ripperda, and S. Staelens, in *Recent Progress on Gravity Tests: Challenges and Future Perspectives*, edited by C. Bambi and A. Cárdenas-Avendaño (Springer, New York, 2024).
[8] J. M. Bardeen, in *Black Holes (Les Astres Occlus)*, edited by C. Dewitt and B. S. Dewitt (Gordon and Breach Science Publishers, New York, 1973), pp. 215–239.
[9] S. E. Gralla and A. Lupsasca, Phys. Rev. D **101**, 044031 (2020).
[10] E. Teo, Gen. Relativ. Gravit. **35**, 1909 (2003).
[11] S. Hadar, M. D. Johnson, A. Lupsasca, and G. N. Wong, Phys. Rev. D **103**, 104038 (2021).
[12] K. Akiyama *et al.* (Event Horizon Telescope Collaboration), Astrophys. J. Lett. **875**, L1 (2019).
[13] K. Akiyama *et al.* (Event Horizon Telescope Collaboration), Astron. Astrophys. **681**, A79 (2024).
[14] K. Akiyama *et al.* (Event Horizon Telescope Collaboration), Astrophys. J. Lett. **930**, L12 (2022).
[15] L. I. Gurvits *et al.*, Acta Astro. **196**, 314 (2022).
[16] P. Kurczynski *et al.*, in *The Event Horizon Explorer mission concept*, Proc. SPIE 12180, Space Telescopes and Instrumentation 2022: Optical, Infrared, and Millimeter Wave (2022) p. 121800M.
[17] V. Kudriashov *et al.*, Chin. J. Space Sci. **41**, 211 (2021).
[18] M.-H. Ulrich, L. Maraschi, and C. M. Urry, Annu. Rev. Astron. Astrophys. **35**, 445 (1997).
[19] R. A. Remillard and J. E. McClintock, Annu. Rev. Astron. Astrophys. **44**, 49 (2006).
[20] E. Berger, Annu. Rev. Astron. Astrophys. **52**, 43 (2014).
[21] K. Fukumura and D. Kazanas, Astrophys. J. **679**, 1413 (2008).

[22] K. Moriyama, S. Mineshige, M. Honma, and K. Akiyama, Astrophys. J. **887**, 227 (2019).
[23] P. M. Chesler, L. Blackburn, S. S. Doeleman, M. D. Johnson, J. M. Moran, R. Narayan, and M. Wielgus, Classical Quantum Gravity **38**, 125006 (2021).
[24] G. N. Wong, Astrophys. J. **909**, 217 (2021).
[25] S. Hadar, S. Harikesh, and D. Chelouche, Phys. Rev. D **107**, 124057 (2023).
[26] J. Dexter, B. Kelly, G. C. Bower, D. P. Marrone, J. Stone, and R. Plambeck, Mon. Not. R. Astron. Soc. **442**, 2797 (2014).
[27] M. Wielgus *et al.* (Event Horizon Telescope Collaboration), Astrophys. J. Lett. **930**, L19 (2022).
[28] See Supplemental Material at http://link.aps.org/supplemental/10.1103/PhysRevLett.133.131402 for further details on the variation of the photon ring critical parameters with black hole spin and inclination, our simulation schemes of black hole movies and Gaussian random fields, the autocorrelation from observations of Sagittarius A*, and the power spectrum of light curve autocorrelations, which includes Refs. [29–35].
[29] D. R. Wilkins, L. C. Gallo, E. Costantini, W. N. Brandt, and R. D. Blandford, Nature (London) **595**, 657 (2021).
[30] S. E. Gralla, A. Lupsasca, and D. P. Marrone, Phys. Rev. D **102**, 124004 (2020).
[31] A. Chael, M. D. Johnson, and A. Lupsasca, Astrophys. J. **918**, 6 (2021).
[32] H. Paugnat, A. Lupsasca, F. H. Vincent, and M. Wielgus, Astron. Astrophys. **668**, A11 (2022).
[33] C. T. Cunningham, Astrophys. J. **202**, 788 (1975).
[34] F. Lindgren, H. v. Rue, and J. Lindström, J. R. Stat. Soc. Ser. B **73**, 423 (2011).
[35] G.-A. Fuglstad, F. Lindgren, D. Simpson, and H. Rue, Statistica Sinica **25**, 115 (2015).
[36] O. Porth, Y. Mizuno, Z. Younsi, and C. M. Fromm, Mon. Not. R. Astron. Soc. **502**, 2023 (2021).
[37] N. S. Conroy, M. Bauböck, V. Dhruv, D. Lee, A. E. Broderick, C.-k. Chan, B. Georgiev, A. V. Joshi, B. Prather, and C. F. Gammie, Astrophys. J. **951**, 46 (2023).
[38] Gravity Collaboration, Astron. Astrophys. **684**, A200 (2024).
[39] D. Lee and C. F. Gammie, Astrophys. J. **906**, 39 (2021).
[40] A. Cárdenas-Avendaño, A. Lupsasca, and H. Zhu, Phys. Rev. D **107**, 043030 (2023).
[41] G. N. Wong, L. Medeiros, A. Cárdenas-Avendaño, and J. M. Stone, Measuring Black Hole Light Echoes with Very Long Baseline Interferometry (to be published).
[42] G. N. Wong, B. S. Prather, V. Dhruv *et al.*, Astrophys. J. Suppl. Ser. **259**, 64 (2022).
[43] J. Lehar, J. N. Hewitt, D. H. Roberts, and B. F. Burke, Astrophys. J. **384**, 453 (1992).
[44] R. A. Edelson and J. H. Krolik, Astrophys. J. **333**, 646 (1988).
[45] C. E. Rasmussen and C. K. I. Williams, *Gaussian Processes for Machine Learning* (MIT Press, Cambridge, MA, 2006).